BIOCHEMISTRY
including biophysical chemistry & molecular biology

Article

pubs.acs.org/biochemistry

Membrane Interactions of the Amphipathic Amino Terminus of Huntingtin

Matthias Michalek, Evgeniy S. Salnikov, Sebastiaan Werten, and Burkhard Bechinger*

Membrane Biophysics and NMR Chemistry Institute UMR7177, University of Strasbourg/CNRS International Center for Frontier Research in Chemistry, 1 rue Blaise Pascal, F-67000 Strasbourg, France

Supporting Information

ABSTRACT: The amino-terminal domain of huntingtin (Htt17), located immediately upstream of the decisive polyglutamine tract, strongly influences important properties of this large protein and thereby the development of Huntington's disease. Htt17 markedly increases polyglutamine aggregation rates and the level of huntingtin's interactions with biological membranes. Htt17 adopts a largely helical conformation in the presence of membranes, and this structural transition was used to quantitatively analyze membrane association as a function of lipid composition. The apparent membrane partitioning constants increased in the presence of anionic lipids but decreased with increasing amounts of cholesterol. When membrane permeabilization was tested, a pronounced dye release was observed from 1-palmitoyl-2-oleoyl-*sn*-glycero-3-phosphocholine (POPC) vesicles and 75:25 (molar ratio) POPC/1-palmitoyl-2-oleoyl-*sn*-glycero-3-phospho-L-serine vesicles but not across bilayers that better mimic cellular membranes. Solid-state nuclear magnetic resonance structural investigations indicated that the Htt17 α-helix adopts an alignment parallel to the membrane surface, and that the tilt angle (~75°) was nearly constant in all of the membranes that were investigated. Furthermore, the addition of Htt17 resulted in a decrease in the lipid order parameter in all of the membranes that were investigated. The lipid interactions of Htt17 have pivotal implications for membrane anchoring and functional properties of huntingtin and concomitantly the development of the disease.

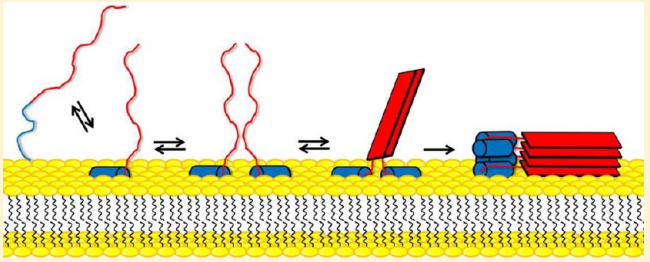

The human gene product huntingtin is the causative agent in the establishment of Huntington's disease. The switch from healthy to pathogenic huntingtin occurs via the multiplication of CAG repeats within the gene. An elongated polyQ tract at the amino terminus of the protein results from the coding of more than 37 glutamine residues, which leads to the development of Huntington's disease and related diseases.[1−4] Even though the length of the polyglutamine sequence of huntingtin has been identified as the decisive element for the development and progression of Huntington's chorea, the molecular mechanisms of its pathology remain unresolved. It has been proposed that Huntington's disease is triggered by perturbations of neuronal membranes caused by expanded stretches of polyglutamines. In particular, membrane disruption, related to processes observed for other amyloidogenic proteins,[5−7] and the concomitant calcium dysregulation[8] have been foci of investigation.[9] When considering membrane interactions, it is notable that huntingtin or fragments thereof are involved in intracellular vesicle trafficking[10,11] and are associated with the endoplasmic reticulum (ER), the Golgi apparatus, and endosomal vesicles.[8,12] Furthermore, their redistribution between the cytoplasm and the nucleus is affected by the length of the polyglutamine tract.[13−15] Finally, the pathogenesis of Huntington's disease has been associated with mitochondrial malfunction.[16,17] Despite these data as well as the clear correlation between the number of polyglutamines and the outbreak of the disease, a variety of experiments have so far not provided evidence of strong and reproducible membrane interactions or the formation of pore structures by expanded polyQs.

While such investigations were performed on isolated polyglutamines, more recent data underline the fact that the cellular localization of huntingtin is heavily influenced by a domain comprising the first 17 amino acids[8] as well as its regulation by posttranslational modifications within this region.[18] In particular, the important role of mutating serine 13 and 16 within this Htt17 domain to prevent disease pathogenesis has been convincingly demonstrated in transgenic mice.[19] To interact with membranes in vivo, huntingtin requires this Htt17 domain directly preceding the polyglutamine region.[8,12] Htt17 strongly enhances polyglutamine oligomerization[8,12,20−22] and is able to interact with itself as well as with polyglutamines.[22] Furthermore, Htt17 is involved in reciprocal cross-talk between polyglutamines and a number of protein sequences.[21,23−25] Polypeptide sequences exhibiting a tendency to self-aggregate were found to oligomerize when structurally perturbed by flanking polyQ domains, and this oligomerization is dependent on the number of glutamines. Subsequently, the polyglutamines themselves assemble into stable fibrillar structures forming the nucleus for additional aggregation processes.[23−25]

Received: September 28, 2012
Revised: January 10, 2013
Published: January 10, 2013

The ensemble of data suggests that a high local concentration of polyglutamines triggers the conformational transitions necessary for aggregation, protofibril and/or fibril formation, and thereby the causative events in the development and progression of Huntington's disease. Although protein-mediated interactions of polyglutamines have been studied in detail,[23−25] the effect of the local accumulation of polyglutamines at bilayer surfaces has so far not been investigated. In particular, Htt17 is involved in huntingtin−membrane interactions when at the same time it is known to enhance polyglutamine aggregation.[8,12,20−22] In vitro and in vivo experiments[8,12,26] strongly suggest a key role for Htt17 in the membrane targeting and interactions of huntingtin as a whole, or of its exon 1 expression and proteolytic cleavage products.[8,13,18,27] Nevertheless, very few data that characterize the functional interactions of Htt17 with membranes or its bilayer-associated conformations are available.

This prompted us to investigate in detail the membrane interactions of Htt17 and two variants of the sequence, Htt17-M8P and P-Htt17, using a number of biophysical approaches. Whereas we were able to study the conformational transition of Htt17 upon membrane association and measure the corresponding partitioning constants by CD spectroscopy, solid-state NMR spectroscopy is a well-established method for determining the topology of polypeptides when associated with phospholipid bilayers.[28,29] We were thereby able to analyze the functional association of Htt17 with lipid bilayers as well as its structural transition in quantitative detail upon translocation from the aqueous phase to a membrane-associated state. The results reveal a pronounced dependence of the Htt17 functional activities and dynamics on the membrane lipid composition and accentuate its role as a lipid binding and membrane targeting domain.

MATERIALS AND METHODS

Amino acid derivatives and other reagents for peptide synthesis were from Novabiochem-Merck (Darmstadt, Germany). All lipids were from Avanti Polar Lipids (Alabaster, AL).

Peptide Synthesis of Specifically Labeled Htt17 Peptides. The Htt17 peptide and its labeled derivatives [^{15}N-Leu^{7},^{2}H$_3$-Ala^{10}]-P-Htt17 and [^{15}N-Leu^{14},^{2}H$_3$-Ala^{10}]-P-Htt17 were prepared by automated solid-phase peptide synthesis using a Millipore 9050 synthesizer and Fmoc (9-fluorenylmethyloxycarbonyl) chemistry. Peptides were purified by semipreparative high-performance liquid chromatography. The Htt17 sequences (MATLEK**L**MK**A**FES**L**KSF) as well as the analogue carrying a mutation of Met^{8} to proline (Htt17-M8P) (cf. ref 12) were prepared with an amidated carboxy terminus. The sequence with an additional proline at its amino terminus (P-Htt17) was included in this study, and its structure and topology were compared to those of Htt17, as the proline derivative is also a result of the bacterial expression as a fusion protein, chemical cleavage, and purification following a previously established protocol for membrane-active peptides.[30] This peptide carries a free carboxy terminus to match as closely as possible the biochemically prepared product.

At the positions shown in bold in the sequence, the natural abundance Fmoc-protected amino acid derivatives (Bachem, Heidelberg, Germany, and Applied Biosystems, Weiterstadt, Germany) were replaced with their isotopically enriched analogues in the [^{15}N-Leu^{7},^{2}H$_3$-Ala^{10}]-P-Htt17 and [^{15}N-Leu^{14},^{2}H$_3$-Ala^{10}]-P-Htt17 sequences (eurisotope, Paris, France). The identity and high purity of the products (>90%) were confirmed by matrix-assisted laser desorption ionization time-of-flight mass spectrometry. After lyophilization, the TFA counterions were exchanged twice with 5% (v/v) acetate. All peptides were exposed to a HFIP/TFA mixture for disaggregation and lyophilized and the TFA counterions exchanged by two treatments of dissolution in 4% (v/v) acetic acid, followed by lyophilization. Prior to functional assays or CD or NMR measurements, the peptides were dissolved in a solvent/buffer mixture.[31] Size-exclusion chromatography was used to confirm the monomeric state of the peptide.

Calcein Release Assay. The effect of Htt17 on model membranes was studied using a calcein release assay.[32] Large unilamellar vesicles (LUVs) were prepared from POPC or POPC/POPS (75:25 molar ratio), POPE/POPG (75:25 molar ratio), or POPC/POPS (75:25 molar ratio) mixtures with increasing cholesterol concentrations of 0, 10, 20, 30, 40, and 50 mol %. Lyophilized peptide was dissolved in 100% (v/v) formic acid to a final concentration of 5 mg/mL. From the peptide stock solution, aliquots were added to 1 mL of 50 mM sodium phosphate buffer, 75 mM sodium chloride, and 1 mM EDTA (pH 7.3) containing LUVs with a defined lipid composition. The fluorescence measurements were performed as described previously.[32] Each experiment was repeated three times; the results were fit to a sigmoidal function, and the standard deviation is indicated in the figures.

Circular Dichroism Spectropolarimetry and Membrane Partitioning Analysis. Circular dichroism spectropolarimetry was performed in 50 mM sodium phosphate buffer and 75 mM sodium chloride (pH 7.3) following protocols described in ref 33. The spectral changes upon titration of vesicles or micelles were used to analyze the apparent membrane partitioning equilibria.[34] Assuming a bilayer partitioning model, the fraction of membrane-associated peptide is calculated according to

$$\text{bound peptide}\,(\%) = [C_{\text{lipid}}/(C_{\text{lipid}} + 1/K_{\text{p}})] \times 100$$

where C_{lipid} is the concentration of phospholipids and K_{p} is the membrane partitioning constant.[35]

Solid-State NMR Spectroscopy. Samples for solid-state NMR spectroscopy were prepared by dissolving 7 mg of Htt17 or P-Htt17 in 100% formic acid and approximately 100 mg of lipid in HFIP. Both solutions were mixed and carefully applied onto 25 ultrathin cover glasses (8 mm × 22 mm, Paul Marienfeld GmbH & Co. KG, Lauda-Königshofen, Germany) as described previously.[36] Care was taken to reduce the organic solvent exposure time to a minimum and to remove all organic solvent under high vacuum. Thereafter, ^{2}H-depleted water (10^{-2} of natural abundance, Aldrich Chemical Co., Milwaukee, WI) was used for sample equilibration at 93% relative humidity.

Solid-state NMR spectra were recorded on a Bruker Avance wide-bore NMR spectrometer operating at 9.4 T. A commercial double-resonance solid-state NMR probe modified with flattened coils with dimensions of 15 mm × 4 mm × 9 mm was used. Proton-decoupled ^{15}N solid-state NMR spectra were acquired using a cross-polarization sequence and processed as described previously.[37] NH_4Cl (40.0 ppm) was used as an external reference corresponding to 0 ppm for liquid NH_3. An exponential apodization function corresponding to a line broadening of 50 Hz was applied before Fourier transformation.

Deuterium solid-state NMR spectra were recorded using a quadrupolar echo pulse sequence.[38] The spectra were referenced relative to $^{2}H_2O$ (0 ppm). An exponential apodization function corresponding to a line broadening of 300 Hz [peptide spectra (Figure 3)] or 10 Hz [lipid spectra (Figure 5)] was applied

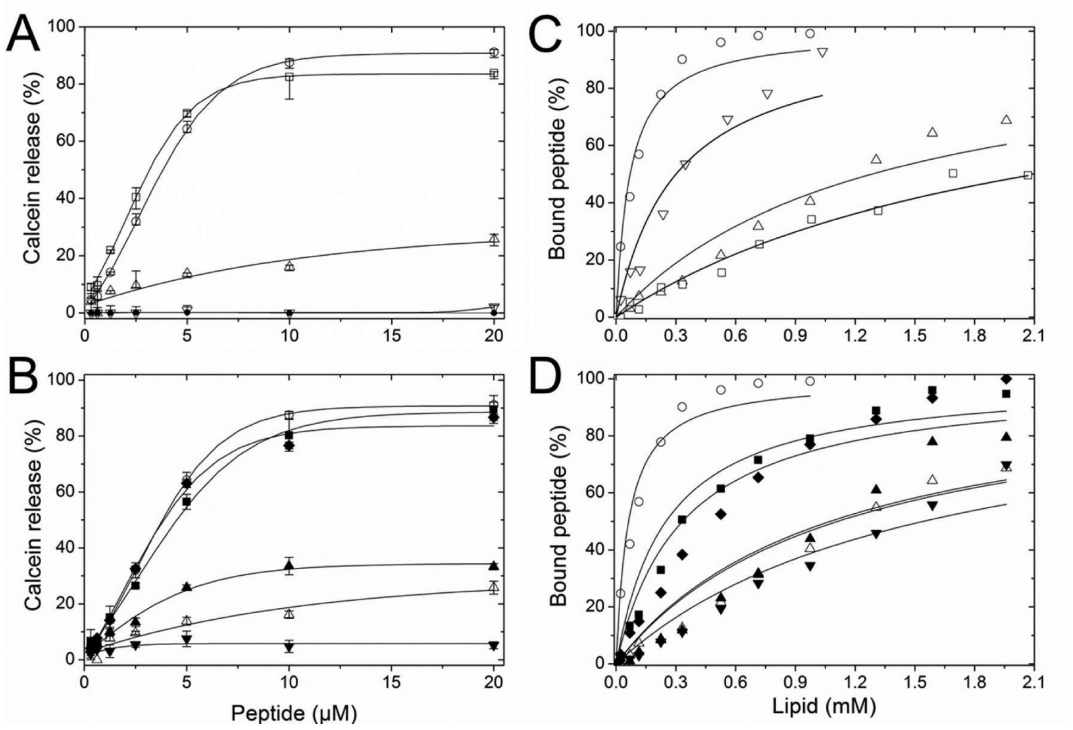

Figure 1. (A) Release of calcein from large unilamellar vesicles in the presence of increasing amounts of Htt17 at 293 K. POPC (□), 75:25 (molar ratio) POPC/POPS (○), 45:15:40 (molar ratio) POPC/POPS/cholesterol (△), or 75:25 (molar ratio) POPE/POPG (▽) LUVs were used. The release from 75:25 (molar ratio) POPC/POPS vesicles in the presence of Htt17-M8P is shown as a control (●). (B) Htt17-induced release from 75:25 (molar ratio) POPC/POPS vesicles (○) with increasing cholesterol ratios of 10 (■), 20 (◆), 30 (▲), 40 (△), and 50% (▼). For comparison, the POPC/POPS data of panel A are also shown in panel B. In all cases, the lipid concentration was 16 μM. (C) Binding isotherm of Htt17 in the presence of POPC, 75:25 (molar ratio) POPC/POPS, 45:15:40 (molar ratio) POPC/POPS/cholesterol, and 75:25 (molar ratio) POPE/POPG vesicles and (D) 75:25 (molar ratio) POPC/POPS vesicles with increasing concentrations of cholesterol derived from the random coil-to-helix transitions. The same symbols as in panels A and B are used. The data were analyzed as described in Materials and Methods.

before Fourier transformation. The deuterium order parameters are analyzed following the method described in ref 39.

Proton-decoupled solid-state ^{31}P NMR spectra were recorded using a Hahn-echo pulse sequence as described previously[37] and referenced relative to 85% phosphoric acid (0 ppm).

Calculation of Orientational Restraints from the Solid-State NMR Spectra. To evaluate the peptide orientations that agree with the experimental spectra, we defined a coordinate system with the tilt angle being the angle between the long axis of the helix and the membrane normal and a pitch angle between the membrane normal and the line within the arbitrary plane of peptide helical wheel projection (cf. Figure 4B for angle definitions). The calculations were performed using the ^{15}N chemical shift main tensor elements at 56, 81, and 223 ppm[40] and 74 kHz for the maximal quadrupolar splitting for the alanine $^{2}H_3C$ group at room temperature.[41] The coordinates of residues 5−17 of low-energy conformer 3 obtained by solution NMR in the presence of DPC micelles were used for this analysis (PDB entry 2LD2; M. Michalek, E. S. Salnikov, and B. Bechinger, unpublished observations). This conformer was chosen as it matches best a series of four solid-state NMR angular restraints obtained from Htt17 in oriented POPC (cf. Table 2). By successively changing the tilt and pitch angles in 50 × 50 steps, we systematically screened the three-dimensional topological space and calculated the corresponding ^{15}N chemical shift and quadrupolar splitting.[38] Wobbling motions of the helix (10° Gaussian distribution) and azimuthal fluctuations around the helix long axis (18°) were assumed to occur independent of each other and were taken into account by averaging the resonance values on the ensemble of orientations with corresponding Gaussian distributions. Such dynamics are similar or closely related to motional regimes that have been found to describe best the dynamics of amphipathic peptides of related dimensions (e.g., ref 42). Contour plots mark the angular restrictions that agree with the experimental results.

RESULTS

Htt17 Permeabilizes Large Unilamellar Vesicles in a Lipid-Dependent Manner. To test the functional activity of the Htt17 domain, a dye release assay was performed using large unilamellar vesicles loaded with 30 mM calcein. At this high concentration, self-quenching of the fluorescent dye occurs, which is relieved upon release from the vesicles. The effect of addition of Htt17 on calcein-entrapped lipid vesicles was quantitatively evaluated by calculating the release of the dye when compared to the absence of peptide (0% release) or the addition of detergent (100% release). In panels A and B of Figure 1, the calcein release as a function of Htt17 concentration and of membrane composition is shown. The most pronounced membrane destabilization is observed for POPC or 75:25 (molar ratio) POPC/POPS vesicles at peptide concentrations of ≥10 μM, but the level of membrane permeabilization by Htt17 is reduced upon addition of cholesterol (Figure 1B). Finally, 75:25 (molar ratio) POPE/POPG vesicles are not affected by the presence of Htt17 (at 25 or 37 °C). As a control, Htt17-M8P was used as this mutation has been shown to result in a reduced level of ER targeting and constitutive nuclear entry of huntingtin.[12] This sequence modification completely abolished calcein release

dx.doi.org/10.1021/bi301325q | Biochemistry 2013, 52, 847−858

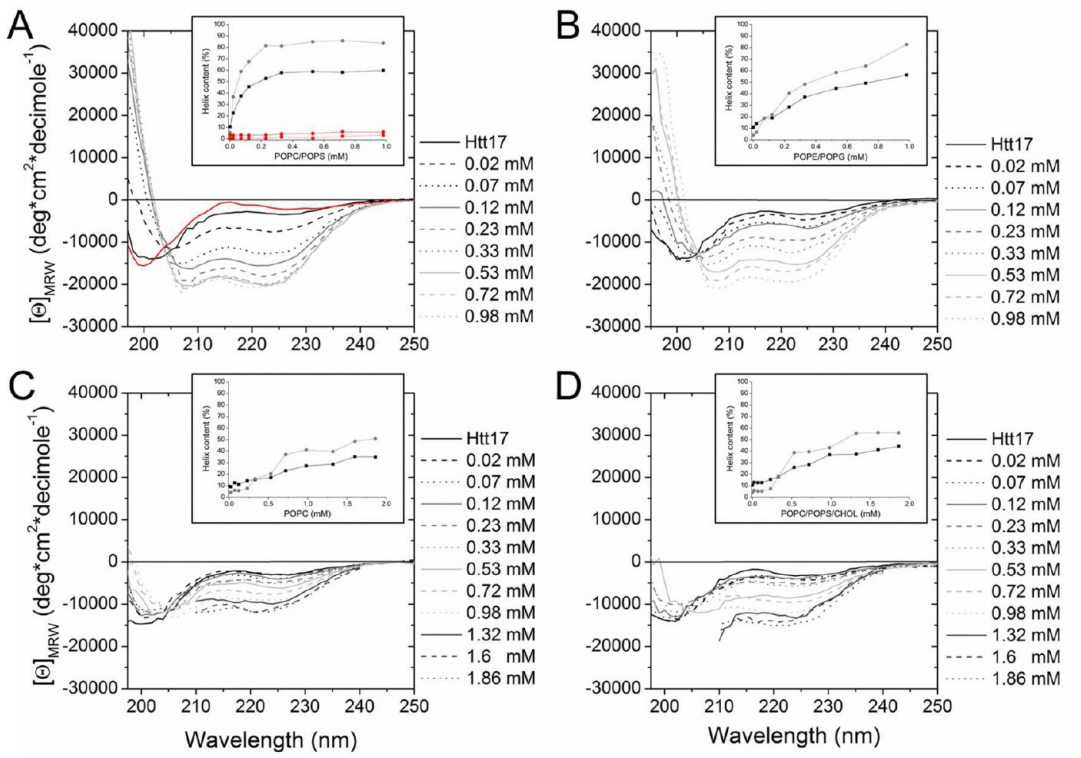

Figure 2. CD spectra of 36 μM Htt17 measured in presence of increasing amounts of 75:25 (molar ratio) POPC/POPS (A), 75:25 (molar ratio) POPE/POPG (B), POPC (C), and (D) 45:15:40 (molar ratio) POPC/POPS/cholesterol small unilamellar vesicles. The insets show the α-helix contents calculated from the ellipticity at 222 nm[60] (black) or by deconvolution of the full spectra using CDSSTR[61] (gray). At high lipid concentrations, light scattering limited the measurements for panels C and D to wavelengths of ≥210 nm. The CD spectrum of Htt17-M8P in the presence of 1 mM 75:25 (molar ratio) POPC/POPS vesicles and the helical contents upon vesicle addition are depicted in panel A (red).

with 75:25 (molar ratio) POPC/POPS vesicles (Figure 1A) or POPC vesicles (data not shown).

Quantitative Evaluation of the Membrane Association of Htt17. Whereas the presence of anionic lipids augments membrane association and thereby the membrane activities of a number of cationic amphipathic peptides,[43] such an increased level of membrane permeabilization is not observed for Htt17 (Figure 1A). Therefore, we also determined the constant for partitioning of Htt17 into membranes as a function of lipid composition. To this end, we monitored the random coil-to-helix transition of Htt17 upon interaction with lipid bilayers using CD spectroscopy.[12] Such circular dichroism experiments at the same time provide insight into the overall secondary structure of membrane-associated Htt17 (Figure 2). Whereas in aqueous buffer the peptide adopts mostly random coil conformations with an helix content of only 10%, this value increases to ~80% upon stepwise addition of 75:25 (molar ratio) POPC/POPS (Figure 2A) or 75:25 (molar ratio) POPE/POPG (Figure 2B) vesicles.

The random coil-to-helix transition as a function of lipid concentration can be used to quantitatively analyze the membrane partitioning of Htt17 and revealed the apparent membrane association constants (cf. Table 1). Furthermore, with an increase in the cholesterol concentration of 3:1 POPC/POPS vesicles, the extent of membrane partitioning of Htt17 decreased (Figure 1D). This effect becomes apparent in the presence of as little as 10% cholesterol, and at 30% cholesterol, the level of partitioning of the peptide is dramatically lowered to within a range that is comparable to that of the interaction of Htt17 with zwitterionic POPC vesicles (Figure 1C and Table 1). Therefore, in these samples even at the highest lipid concentrations tested (>1 mM), the CD spectra represent contributions from both free

Table 1. Apparent Membrane Partitioning Constants of Htt17 with SUVs as a Function of Lipid Composition at 25 °C

lipid composition (molar ratios)	K_p (M^{-1})
3:1 POPE/POPG	3319 ± 476
POPC	484 ± 23
3:1 POPC/POPS	20476 ± 2578
3:1 POPC/POPS with 10% cholesterol	3150 ± 358
3:1 POPC/POPS with 20% cholesterol	2531 ± 355
3:1 POPC/POPS with 30% cholesterol	930 ± 143
3:1 POPC/POPS with 40% cholesterol	777 ± 71
3:1 POPC/POPS with 50% cholesterol	649 ± 63

(mostly random coil) and bound (mostly helical) peptide conformations, with the ratio being dependent on the detailed lipid composition. Finally, the CD spectra of the Htt17-M8P peptide indicate a largely random coil conformation that does not change even upon addition of 1 mM 3:1 POPC/POPS vesicles (Figure 2A) or 1 mM POPC vesicles (data not shown). These data and the complete loss of membrane permeabilization (Figure 1A) suggest that an expanded amphipathic helical structure is a prerequisite for efficient membrane interactions.

Topological and Structural Analysis of Bilayer-Associated Htt17 by Oriented Solid-State NMR Spectroscopy. To study the interactions of Htt17 with phospholipid bilayers, Htt17 sequences were prepared by solid-phase peptide synthesis with ^{15}N isotopes at position 7 or 14 and ^{2}H isotopes at position 10. The peptides were reconstituted into oriented phospholipid bilayers, and solid-state NMR spectra were recorded (Figure 3). Because of the unique properties of the ^{15}N amide chemical shift tensor, the ^{15}N chemical shift of backbone-labeled polypeptides

dx.doi.org/10.1021/bi301325q | Biochemistry 2013, 52, 847−858

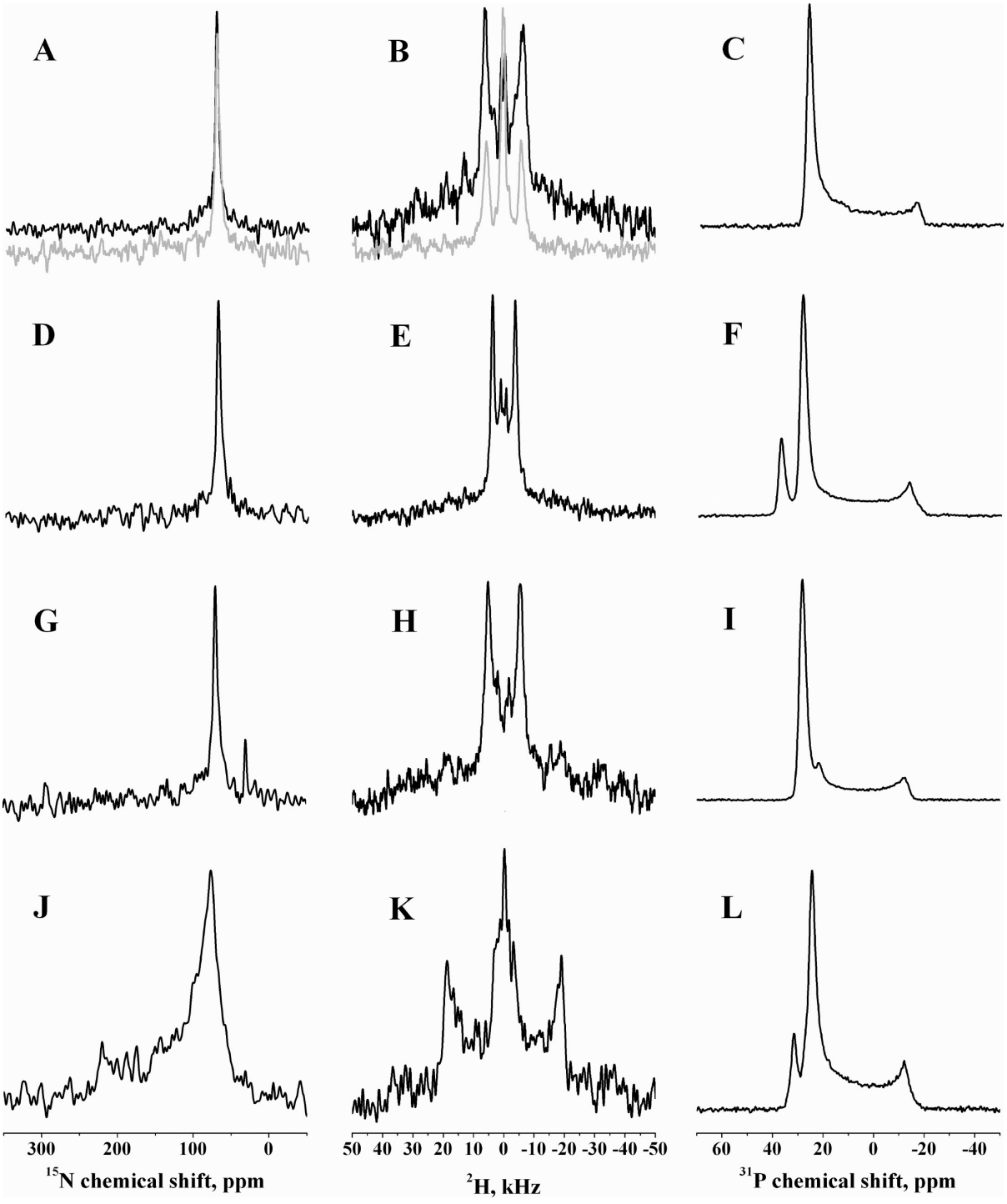

Figure 3. Proton-decoupled ^{15}N (A, D, G, and J), ^{2}H (B, E, H, and K), and proton-decoupled ^{31}P solid-state NMR spectra (C, F, I, and L) of oriented membrane samples carrying 2.5 mol % [^{15}N-Leu^{7},$^{2}H_3$-Ala^{10}]-P-Htt17. POPC (A–C), 75:25 POPC/POPS (D–F), 75:25 POPE/POPG (G–I) and 45:15:40 POPC/POPS/cholesterol (J–L) membranes were used (lipid molar ratios are provided). The spectra shown in gray in panels A and B are from [^{15}N-Leu^{7},$^{2}H_3$-Ala^{10}]-Htt17 in oriented POPC membranes (note that ^{2}H natural abundance water was used for equilibrating this sample).

provides a direct measure of the approximate tilt angle of the helical domain.[44] Whereas transmembrane helical alignments are characterized by ^{15}N chemical shifts in the 200 ppm region, α-helices that are oriented parallel to the membrane surface exhibit values of <100 ppm. These data are ideally complemented by measurements of the quadrupolar splitting of methyl-deuterated alanines where the combination of ^{15}N and ^{2}H spectra provides accurate rotational pitch and tilt angle information.[29,38]

Previously, we investigated the membrane structure and topology of Htt17 in DPC micelles and POPC bilayers by multidimensional solution and solid-state NMR spectroscopy, respectively (M. Michalek, E. S. Salnikov, and B. Bechinger, unpublished observations). The data indicate that in membrane environments Htt17 adopts an α-helical conformation between residues 6 and 17. By selecting from the NMR conformational ensemble in micellar environments (PDB entry 2LD2) those

dx.doi.org/10.1021/bi301325q | *Biochemistry* 2013, 52, 847–858

structures that best fit the solid-state NMR angular restraints (Table 2), we obtained a refined structure in POPC phospholipid

Table 2. ^{15}N and ^{2}H Solid-State NMR Measurements of Htt17 and P-Htt17 in Oriented Phospholipid Bilayers[a]

	POPC	3:1 POPC/POPS	3:1 POPE/POPG
[^{15}N-Leu^{7}]-P-Htt17	72 ± 1.7 ppm[b]	69 ± 2 ppm[b]	70 ± 2 ppm[b]
[^{15}N-Leu^{7}]Htt17	71.2 ± 1.7 ppm		
[$^{2}H_3$-Ala^{10}]-P-Htt17	11.5 ± 2.5 kHz[b]	7.5 ± 1.2 kHz[b]	11 ± 1.5 kHz[b]
[$^{2}H_3$-Ala^{10}] Htt17	11 ± 2.5 kHz		
[^{15}N-Phe^{11}] Htt17	78.9 ± 1.5 ppm	77.6 ± 1.2 ppm[c]	
[^{15}N-Leu^{14}]-P-Htt17	73.3 ± 1.2 ppm[c]	73.2 ± 1.2 ppm[c]	
[^{15}N-Phe^{17}] Htt17	88.2 ± 0.9 ppm	89.8 ± 1.0 ppm[c]	

[a]The error bars are estimated from the line width at 80% height. [b]Spectra are shown in Figure 3. [c]Spectra are shown in Figure S1 of the Supporting Information.

bilayers. Furthermore, the combination of four solid-state NMR orientational restraints results in a unique topology of Htt17 in this phospholipid bilayer characterized by tilt and rotational pitch angles of 103 ± 5° and 137 ± 5°, respectively, in accordance with its amphipathic character.

Here, we investigated an additional labeling position (Leu^{14}), and to gain structural insight into the lipid dependence of Htt17 membrane permeabilization (Figure 1A), we performed complementary solid-state NMR experiments in oriented membranes that have a lipid composition identical to the composition of those used for the calcein release assays. Representative spectra are shown in Figure 3 and Figure S1 of the Supporting Information, and the data are summarized in Table 2. Whereas the ^{15}N chemical shift of Leu^{7} remains unaltered (71 ± 2 ppm) upon comparison of POPC, 75:25 POPC/POPS, and 75:25 POPE/POPG membranes (Figure 3A,D,G), the differences are somewhat more pronounced for the $^{2}H_3$-Ala^{10}-labeled site. The deuterium quadrupolar splitting of this site equals 11.5 ± 2.5 kHz when Htt17 is reconstituted into POPC vesicles (Figure 3B), 7.5 ± 1.2 kHz in the presence of 75:25 POPC/POPS vesicles (Figure 3E), and 11.0 ± 1.5 kHz in the presence of 75:25 POPE/POPG vesicles (Figure 3H). When the peptide labeled at the Leu^{14} position was investigated, ^{15}N chemical shifts of 73 ppm were obtained in both POPC and 75:25 POPC/POPS phospholipid bilayers (Figure S1A,D of the Supporting Information and Table 2). In contrast, the ^{15}N and ^{2}H spectra recorded in the cholesterol-containing membranes reveal features that closely resemble those of nonoriented peptides (Figure 3J,K), probably as this stiffer membrane does not allow for efficient membrane insertion (Figure 1D) and thereby alignment of Htt17.

The spectra shown in Figure 3 were recorded from an Htt17 variant carrying an additional proline residue at the amino terminus. This peptide was included in this study and directly compared to Htt17 because this sequence variation results from a bacterial overexpression and purification system that we recently developed to produce isotopically labeled membrane-active peptides for heteronuclear NMR.[30] Upon comparison of the spectra obtained from P-Htt17 in POPC bilayers (Figure 3A,B, black lines), Htt17 yields ^{15}N chemical shifts and ^{2}H quadrupolar splittings that are identical within experimental error (Figure 3A,B, gray lines; 71.0 ± 2.5 ppm for ^{15}N-Leu^{7} and 11 ± 2.5 kHz for $^{2}H_3$-Ala^{10}), indicating that the additional proline and the carboxy-terminal protection have an only minor effect on the topology of the helical domain. Notably, the chemical shifts of Leu^{7} and Phe^{17} (Figure 3A,D,G and Figure S1C,F of the Supporting Information and Table 2), far from the isotropic value (120 ppm) indicate that these residues undergo little motion despite their localization at the helical boundaries in the micellar structure.

The angular constraints obtained from the NMR measurements (Table 2) restrict the possible helix orientations relative to the membrane normal, and this was analyzed in quantitative detail.[29,45,46] The topological analysis of Figure 4 represents all possible peptide alignments in the membrane. Whenever the calculated and experimental values match (including experimental uncertainties), the combination of tilt and orientational pitch angles is highlighted in the corresponding topology graph that is shown in Figure 4A for the data obtained in oriented POPC bilayers (Figure 3A,B and Table 2). The restriction plots that arise in this manner for the ^{15}N chemical shift of Leu^{7} and Leu^{14} as well as the ^{2}H quadrupolar splitting of Ala^{10} are shown as red, violet, and black traces, respectively. The intersections arising from the ^{15}N chemical shift of Leu^{7} and the ^{2}H quadrupolar splitting of Ala^{10} leave only four possible helix alignments in the membrane (intersections between the red and black traces in Figure 4A,C,D), thereby indicating the highly complementary nature of these two constraints.[38] Adding the angular information obtained from the ^{15}N-Leu^{14} chemical shift (Figure S1A of the Supporting Information) eliminates two of these possibilities (Figure 4A,C). This leaves two possible solutions, of which topology I (tilt and pitch angles of 105° and 129°, respectively) is energetically favored over topology II (95° and 153°, respectively) when following the approach described in ref 45. The experimental errors are taken into account in Figure 4, to which has to be added the possibility of systematic errors (±5°) due to uncertainties in the description of the individual chemical shift and quadrupolar tensors[40,41] as well as in the details of the motional regime of the membrane-associated peptides (E. S. Salnikov, M. Michalek, and B. Bechinger, unpublished observations). Therefore, the topology of P-Htt17 in POPC (Figure 4A,B) is within experimental error identical to that of Htt17 in the same lipid unambiguously derived from four orientational restraints for Htt17 (Table 2) in the same oriented phospholipid bilayer (103° and 137°, respectively; M. Michalek, E. S. Salnikov, and B. Bechinger, unpublished observations).

Even though the experimental data set does not allow one to unambiguously determine the topology, the similarity of the NMR spectra (Figure 3 and Figure of the Supporting Information) and of the topology plots (Figure 4) suggests that the following tilt and pitch angular pairs represent the membrane topology of P-Htt17 in POPC [105°/129° (Figure 4A,B)], 75:25 POPC/POPS [105°/125° (Figure 4C)], and 75:25 POPE/POPG [105°/130° (Figure 4D)] vesicles. Although the POPC and POPC/POPS membranes exhibit the largest differences in solid-state NMR spectral parameters (Figure 3B,E) and functional properties (Figure 1A,C), the topology of the helix differs only marginally (<10°).

Furthermore, the proton-decoupled ^{31}P solid-state NMR spectra of the same samples used for the topological analysis are shown in panels C, F, I, and L of Figure 3. The spectra are characteristic of liquid disordered bilayers, and the signal at 30 ppm is indicative of a predominant alignment of the

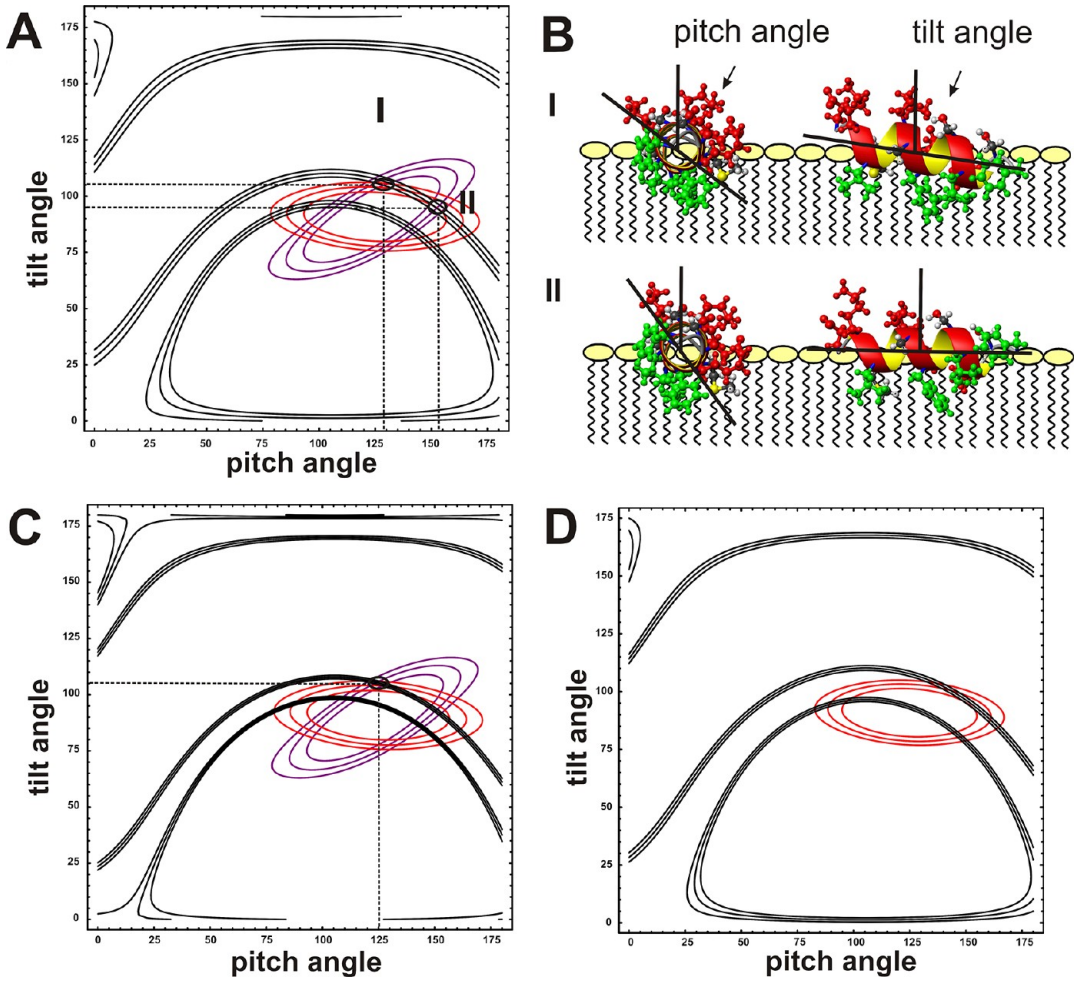

Figure 4. Angular restrictions obtained from solid-state NMR spectra of the Htt17 helix when the peptide is reconstituted in oriented bilayers. The topologies that agree with the experimental ^{2}H quadrupolar splitting of $^{2}H_{3}$-Ala^{10} (black) and the ^{15}N chemical shifts of ^{15}N-Leu^{7} (red) and ^{15}N-Leu^{14} (violet) are shown for (A) POPC, (C) 75:25 POPC/POPS, and (D) 75:25 POPE/POPG membranes. The NMR data shown in Figure 3 and listed in Table 2 were used for this analysis. The three lines for each restriction plot reflect the main resonance intensity as well as the frequencies at half-height. In panel A, the tilt and rotational pitch angles are circled where all experimental data agree, and the corresponding helix domain (residues 5−17) orientations relative to the membrane normal are shown in panel B. Color coding: red for Lys and Glu, green for Leu and Phe, and gray for Ala, Ser, and Met.

phospholipids with their long axes parallel to the membrane normal. The contributions reaching −15 ppm are often observed for in-plane oriented amphipathic helices and have been assigned to membrane thinning and regions of high local curvature.[39]

To complement the CD and solid-state NMR structural analysis of Htt17 in bilayers, the effect of this amphipathic domain on the lipid organization was also investigated. The ^{2}H solid-state NMR spectra of palmitoyl deuterated [$^{2}H_{31}$]POPC, [$^{2}H_{31}$]POPE/POPG, POPE/[$^{2}H_{31}$]POPG, or [$^{2}H_{31}$]POPC/POPS/cholesterol membranes indicate a decrease in the membrane order parameter in all cases (Figure 5). The alterations amount in average to 24% for [$^{2}H_{31}$]POPC (Figure 5A), 25% for [$^{2}H_{31}$]POPE/POPG (Figure 5B), 13% for POPE/[$^{2}H_{31}$]POPG (Figure 5C), 18% for [$^{2}H_{31}$]POPC/POPS (Figure 5D), and 31% for [$^{2}H_{31}$]POPC/POPS/cholesterol (Figure 5E) vesicles. Nearly similar membrane hydrophobic core alterations were observed for [$^{2}H_{31}$]POPC and [$^{2}H_{31}$]POPE/POPG vesicles at 22 °C (data not shown). These data as well as the ^{31}P solid-state NMR spectra recorded from the oriented samples are similar to those in the presence of other in-plane amphipathic peptides causing membrane thinning and regions of high local curvature.[39]

DISCUSSION

Huntingtin is a large protein, for which more than 200 interaction partners have been reported. The mutated gene product of huntingtin has a molecular mass of 350 kDa and is mostly localized in the cytoplasm, but also associated with the nucleus, plasma membrane, ER, Golgi apparatus, endocytic vesicles, and mitochondria.[8,12,13,16,17,47,48] The protein in its altered form and proteolytic fragments thereof[13,27] are responsible for Huntington's disease via their interference with multiple cellular pathways, and among other physiological effects, they cause the malfunctioning of mitochondria and ultimately neuronal degeneration.[49]

Despite clear correlations between the genetic modifications and the onset of Huntington's disease being identified,[49] the biological function and the molecular mechanisms of the development of the pathologies are still under discussion. The analysis of molecular events is hindered by the large number of interaction partners of this protein and the lack of high-

dx.doi.org/10.1021/bi301325q | Biochemistry 2013, 52, 847−858

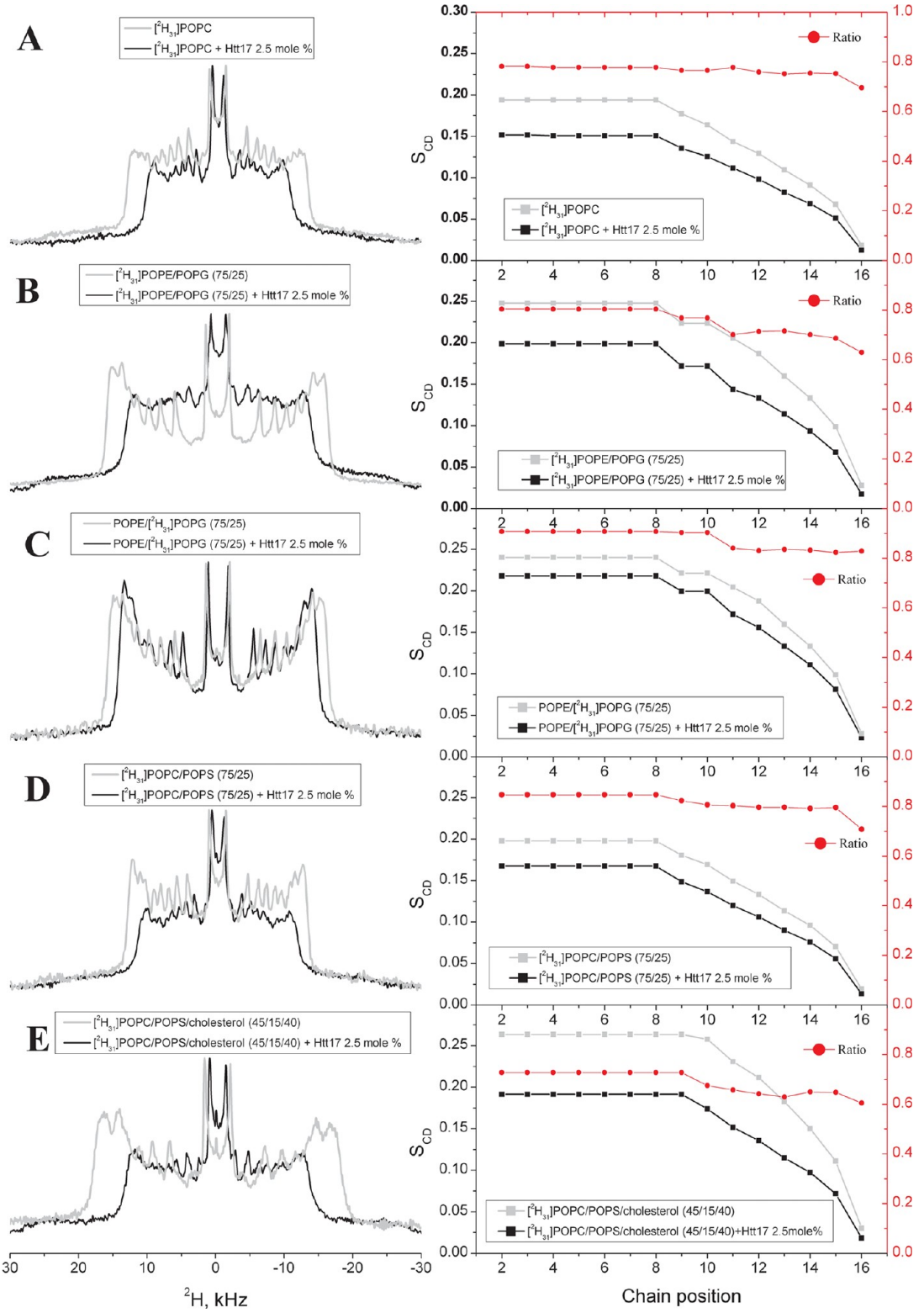

Figure 5. Lipid bilayer packing in the presence of Htt17. Comparison of echo solid-state ^{2}H NMR spectra acquired for lipid bilayers in the absence (gray line) or presence of 2.5 mol % [^{15}N-Phe^{11}]Htt17 (black line) at 37 °C and the corresponding order parameter (S_{CD}) profiles (left axis): (A) [$^2H_{31}$]POPC, (B) 75:25 [$^2H_{31}$]POPE/POPG, (C) 75:25 POPE/[$^2H_{31}$]POPG, (D) 75:25 [$^2H_{31}$]POPC/POPS, and (E) 45:15:40 [$^2H_{31}$]POPC/POPS/cholesterol vesicles (molar ratios are indicated). The red circles depict the S_{CD}(with peptide)/S_{CD}(pure membrane) ratio, i.e., the normalized influence of the peptide on membrane order (right axis).

resolution structural information. Here we demonstrate that the Htt17 domain associates with biological membranes in a strongly lipid-dependent and reversible manner. The data suggest that Htt17 is involved in targeting this large protein to peripheral membrane association sites, where the spatiotemporal redistribution can be part of regulatory mechanisms. Indeed,

dx.doi.org/10.1021/bi301325q | *Biochemistry* 2013, 52, 847−858

huntingtin is found to be associated with a great number of organelles, including the cytoplasm, the nucleus, the plasma membrane, the ER, the Golgi apparatus, endocytic vesicles, and mitochondria.[8,12,13,16,17,47,48] This complexity of interactions makes it difficult to identify the biological functions of huntingtin and the disease-promoting biochemical processes.

Furthermore, the amino-terminal domain encompassing the first 17 amino acids of huntingtin (Htt17) has proven to be tightly linked to polyglutamine aggregation and the resulting toxicity of huntingtin in its pathogenic state.[8,12,21,26] In this work, we demonstrate that Htt17 interacts with lipid bilayers, and as a consequence, these interactions should be considered when the pathological consequences of extended polyglutamines are discussed.

The membrane partitioning of this domain is coupled to a conformational transition from random coil to α-helical (Figure 2). Notably, the peptide also exhibits a helix forming propensity in aqueous solution when being investigated by CD (Figure 2)[12] or solution NMR spectroscopy,[21] and additionally in molecular dynamics simulations[20] as well as in the X-ray crystallographic analysis of an MBP−Htt17−polyQ fusion protein.[50] The CD data indicate that Htt17 forms an amphipathic helical structure covering 70−80% of the peptide in the presence of a great variety of membranes. This is in excellent agreement with the structure in the presence of DPC micelles obtained by multidimensional NMR spectroscopy, which indicates a helical conformation encompassing residues 6−17 (PDB entry 2LD2; M. Michalek, E. S. Salnikov, and B. Bechinger, unpublished observations). Solid-state NMR experiments show that this helical domain is oriented approximately parallel to the surface (tilt angle of ∼75°) in all pure phospholipid membranes investigated here (Figures 3 and 4). This alignment is within experimental error identical for the Htt17 and the P-Htt17 sequences, indicating that modifications of the termini, which are both exposed to the water phase (Figure 4B and unpublished observations of M. Michalek, E. S. Salnikov, and B. Bechinger), have little effect on membrane structure and topology.

Interestingly, the experimentally determined pitch angle of the amphipathic helix is somewhat larger than expected from merely screening the polarity of the side chains (Figure 4B) and places Glu^{12} and Lys^{15} in a membrane (interfacial) environment. We suggest that this localization is stabilized by intra- or intermolecular salt bridge formation. Notably, there is little information about the side chain conformations in bilayer environments, which may be somewhat different when compared to the micelle structure (PDB entry 2LD2). Furthermore, it is possible that the interactions of residues 1−4 with the membrane interface, not considered here, contribute to the bilayer topology. Finally, the Htt17 domain has been shown to form dimers,[22] and this propensity for association may persist in membrane environments (cf. Figure 6) possibly involving the Glu^{12}−Lys^{15} intermolecular salt bridges mentioned above.

The stepwise decrease in the relative order parameter of several membranes at approximately C atoms 8−10 (Figure 5B−E) is in agreement with an interfacial localization of the amphipathic helix at an alignment parallel to the surface.[51,52] Upon addition of cholesterol, the membranes stiffen and the level of association of the peptide with the bilayer gradually decreases (Figures 1B,D and 3J,K and Table 1). Furthermore, the presence of acidic phospholipids augments the apparent membrane partitioning coefficient probably by electrostatic attraction and a concomitantly increased concentration of the overall cationic peptide close to the membrane surface.[53] Interestingly, the apparent level of binding to the 75:25 (molar ratio) POPC/POPS membrane is increased by 1 order of magnitude compared to that with the 75:25 (molar ratio) POPE/POPG membrane (Table 1) and may be due to a number of differences in the interfacial properties of the phospholipids such as hydrogen bonding between PE headgroups, the high gel-to-liquid disordered phase transition temperature of POPE (T_c = 25 °C), the tri-ionic nature of PS, or the molecular shapes[52] and/or phase preferences of the phospholipids.

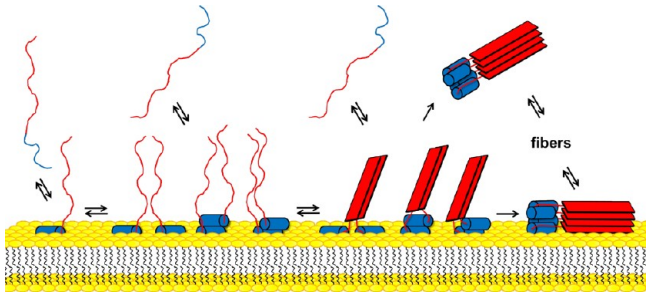

Figure 6. Schematic representation of the possible role of Htt17 in the huntingtin aggregation process. The Htt17 domain (blue) anchors huntingtin at membranes concomitant with a structural transition. The resulting α-helix (cylinder) is oriented along the membrane surface with the C-terminal phenylalanine (Phe^{17}) and the subsequent polyQ tract (red) facing the cytosol. Membrane-associated Htt17 thereby brings polyQ tracts into the proximity, permitting nucleation that is dependent on the length of the glutamine tract, and the formation of extended β-sheets. High-molecular mass aggregates ultimately result in toxic fibril formation and cell death. In addition, the amphipathic character of the α-helix favors interactions with other protein domains.

Although membrane permeabilization has been measured in a quantitative manner for Htt17 (Figure 1A), it is unlikely that this reflects the biologically relevant mechanism of huntingtin because the activity is much reduced in the presence of cholesterol or virtually absent for 75:25 (molar ratio) POPE/POPG vesicles. Notably, increasing the temperature to 37 °C showed no effect on the permeabilization of 75:25 (molar ratio) POPE/POPG membranes by Htt17 (data not shown). Of all membranes investigated, these lipid compositions mimic best eukaryotic plasma membranes and the membranes of mitochondria, respectively. Therefore, the functional data shown in Figure 1 agree with previous observations that indicate that Htt17 is required for the cellular toxicity of huntingtin but not sufficient for cell killing (through membrane permeabilization) in the absence of an extended polyglutamine chain.[8,12,21,26]

However, this lipid dependence of activity is interesting on academic grounds as the most pronounced permeabilization activities are observed for POPC vesicles (Figure 1A) where the level of membrane association is lowest (Figure 1C and Table 1). Furthermore, the changes in membrane order parameter upon addition of Htt17 ($[^2H_{31}]$POPC/POPS/cholesterol > $[^2H_{31}]$POPC ∼ $[^2H_{31}]$POPE/POPG > $[^2H_{31}]$POPC/POPS > POPE/$[^2H_{31}]$POPG) show no correlation to the differences in dye release (POPC ∼ POPC/POPS > POPC/POPS/cholesterol > POPE/POPG). Such a lack of correlation has been reported for other cationic peptides[35,54,55] and suggests that other details such as hydrogen bonding capacity, specific interactions with lipid headgroups, membrane insertion depth, and the resulting curvature strain may be important parameters for explaining membrane permeabilization.[35]

dx.doi.org/10.1021/bi301325q | *Biochemistry* 2013, 52, 847−858

Interestingly, in the 75:25 (molar ratio) POPE/POPG mixture, P-Htt17 exhibits a stronger influence on the zwitterionic [$^2H_{31}$]POPE than on the charged [$^2H_{31}$]POPG lipid (Figure 5B,C). Whereas for cationic peptides electrostatic interactions tend to favor selective interactions with acidic lipids (e.g., ref 56), the net charge of P-Htt17 is rather small and other interactions seem to dominate its membrane interactions.

Recently, it was shown that also in fibrils of exon 1 polypeptides nearly the entire Htt17 domain remains helical despite the polyglutamine tract undergoing a transition into a β-strand conformation.[57] The data presented here suggest that the membrane-induced amphipathic helical structure of Htt17 allows the huntingtin protein to be anchored at the membrane surface.[12,57,58] Thereby, this domain also assures high local concentrations of the associated polyglutamines, which is a prerequisite for aggregation. Posttranslational phosphorylation of the Htt17 domain is expected to weaken the membrane interactions, thereby explaining the decrease in toxicity of huntingtin upon such modification.[18] Additional domains for membrane interaction of huntingtin have been identified in a region proximal to residues 229−249.[10,59] These interactions are of electrostatic nature and farther from the polyglutamine tract and can reinforce the membrane interactions of huntingtin.

A schematic model of how membrane association possibly impacts polyglutamine aggregation is presented in Figure 6 and discussed here. The Htt17 amphipathic structure upon membrane binding is concomitant with an alternation of negative and positive charges along the hydrophilic face of the helix. This structural feature is favorable for homologous interactions between Htt17 monomers but also for mediating heterologous association with polyglutamines, the latter interaction having been suggested to be involved in polyglutamine oligomerization.[21,22] Additionally, it was shown that the chaperonin TriC suppresses huntingtin aggregation by interacting with the Htt17 hydrophobic face whereas externally added Htt17 enhances aggregation probably by intermolecular bridging of polyQ tracts.[22] The membrane anchoring activity of Htt17 can therefore be pivotal in bringing together the polyglutamine domains and, provided that the tracts are sufficiently long, facilitating their oligomerization into toxic association intermediates and fibrils (Figure 6). Notably, the topological arrangement of Htt17 (Figure 4) assures the exposition of the terminal Phe[17] and the subsequent polyglutamines to the water phase. In the case of polyQ aggregation, only small conformational alterations of Htt17 are required as much of the α-helical conformation of Htt17 persists in the fibril.[57] The helical domain, besides its membrane anchoring activity, may therefore also act as a nucleation scaffold initiating the aggregation process.[22] Consequently, the membrane interactions that are described and quantitatively evaluated by the biophysical and structural data presented here delineate novel approaches, which could be used to accelerate therapeutic developments to prevent the disease and to ease the life of Huntington patients.

■ ASSOCIATED CONTENT

Supporting Information

Additional proton-decoupled ^{15}N solid-state NMR spectra of P-Htt17 and Htt17. This material is available free of charge via the Internet at http://pubs.acs.org.

■ AUTHOR INFORMATION

Corresponding Author

*Membrane Biophysics and NMR Chemistry Institute UMR7177, University of Strasbourg/CNRS International Center for Frontier Research in Chemistry, 1 rue Blaise Pascal, F-67000 Strasbourg, France. Telephone: +33 3 68 85 13 03. Fax: +33 3 68 85 17 35. E-mail: bechinge@unistra.fr.

Author Contributions

M.M. and E.S.S. contributed equally to this work.

Funding

We are most grateful for financial support by the CHDI foundation for funding the work through an early discovery initiative and the Deutsche Forschungsgemeinschaft (DFG) for supporting M.M. when he contributed to the early edition of the manuscript. We acknowledge the financial support by the RTRA International Center for Frontier Research in Chemistry, the LabEx Chemistry of Complex Systems (Agence Nationale de la Recherche), the Région Alsace, the University of Strasbourg and the CNRS.

Notes

The authors declare no competing financial interest.

■ ACKNOWLEDGMENTS

We are thankful to Christopher Aisenbrey and Delphine Hatey for technical assistance and valuable discussions.

■ ABBREVIATIONS

CD, circular dichroism; DPC, dodecylphosphocholine; HFIP, 1,1,1,3,3,3-hexafluoro-2-propanol; NMR, nuclear magnetic resonance; PBS, phosphate-buffered saline; PDB, Protein Data Bank; POPC, 1-palmitoyl-2-oleoyl-*sn*-glycero-3-phosphocholine; POPE, 1-palmitoyl-2-oleoyl-*sn*-glycero-3-phosphoethanolamine; POPG, 1-palmitoyl-2-oleoyl-*sn*-glycero-3-phospho(1′-*rac*-glycerol); POPS, 1-palmitoyl-2-oleoyl-*sn*-glycero-3-phospho-L-serine; TFA, trifluoroacetic acid.

■ REFERENCES

(1) Ross, C. A. (2002) Polyglutamine pathogenesis: Emergence of unifying mechanisms for Huntington's disease and related disorders. *Neuron 35*, 819−822.

(2) Rubinsztein, D. C., Leggo, J., Coles, R., Almqvist, E., Biancalana, V., Cassiman, J. J., Chotai, K., Connarty, M., Crauford, D., Curtis, A., Curtis, D., Davidson, M. J., Differ, A. M., Dode, C., Dodge, A., Frontali, M., Ranen, N. G., Stine, O. C., Sherr, M., Abbott, M. H., Franz, M. L., Graham, C. A., Harper, P. S., Hedreen, J. C., Hayden, M. R., et al. (1996) Phenotypic characterization of individuals with 30−40 CAG repeats in the Huntington disease (HD) gene reveals HD cases with 36 repeats and apparently normal elderly individuals with 36−39 repeats. *Am. J. Hum. Genet. 59*, 16−22.

(3) Sathasivam, K., Amaechi, I., Mangiarini, L., and Bates, G. (1997) Identification of an HD patient with a (CAG)180 repeat expansion and the propagation of highly expanded CAG repeats in lambda phage. *Hum. Genet. 99*, 692−695.

(4) Andresen, J. M., Gayan, J., Djousse, L., Roberts, S., Brocklebank, D., Cherny, S. S., Cardon, L. R., Gusella, J. F., MacDonald, M. E., Myers, R. H., Housman, D. E., Wexler, N. S., Grp, U.-V. C. R., and Grp, H. M. C. R. (2007) The relationship between CAG repeat length and age of onset differs for Huntington's disease patients with juvenile onset or adult onset. *Ann. Hum. Genet. 71*, 295−301.

(5) Nanga, R. P. R., Brender, J. R., Vivekanandan, S., Popovych, N., and Ramamoorthy, A. (2009) NMR Structure in a Membrane Environment Reveals Putative Amyloidogenic Regions of the SEVI Precursor Peptide PAP(248−286). *J. Am. Chem. Soc. 131*, 17972−17979.

(6) Brender, J. R., Salamekh, S., and Ramamoorthy, A. (2012) Membrane Disruption and Early Events in the Aggregation of the Diabetes Related Peptide IAPP from a Molecular Perspective. *Acc. Chem. Res. 45*, 454−462.
(7) Sciacca, M. F. M., Kotler, S. A., Brender, J. R., Chen, J., Lee, D. K., and Ramamoorthy, A. (2012) Two-Step Mechanism of Membrane Disruption by Aβ through Membrane Fragmentation and Pore Formation. *Biophys. J. 103*, 702−710.
(8) Rockabrand, E., Slepko, N., Pantalone, A., Nukala, V. N., Kazantsev, A., Marsh, J. L., Sullivan, P. G., Steffan, J. S., Sensi, S. L., and Thompson, L. M. (2007) The first 17 amino acids of Huntingtin modulate its sub-cellular localization, aggregation and effects on calcium homeostasis. *Hum. Mol. Genet. 16*, 61−77.
(9) Monoi, H., Futaki, S., Kugimiya, S., Minakata, H., and Yoshihara, K. (2000) Poly-L-glutamine forms cation channels: Relevance to the pathogenesis of the polyglutamine diseases. *Biophys. J. 78*, 2892−2899.
(10) Kegel, K. B., Sapp, E., Yoder, J., Cuiffo, B., Sobin, L., Kim, Y. J., Qin, Z. H., Hayden, M. R., Aronin, N., Scott, D. L., Isenberg, F., Goldmann, W. H., and DiFiglia, M. (2005) Huntingtin associates with acidic phospholipids at the plasma membrane. *J. Biol. Chem. 280*, 36464−36473.
(11) Valencia, A., Reeves, P. B., Sapp, E., Li, X. Y., Alexander, J., Kegel, K. B., Chase, K., Aronin, N., and DiFiglia, M. (2010) Mutant Huntingtin and Glycogen Synthase Kinase 3-β Accumulate in Neuronal Lipid Rafts of a Presymptomatic Knock-In Mouse Model of Huntington's Disease. *J. Neurosci. Res. 88*, 179−190.
(12) Atwal, R. S., Xia, J., Pinchev, D., Taylor, J., Epand, R. M., and Truant, R. (2007) Huntingtin has a membrane association signal that can modulate huntingtin aggregation, nuclear entry and toxicity. *Hum. Mol. Genet. 16*, 2600−2615.
(13) Tanaka, Y., Igarashi, S., Nakamura, M., Gafni, J., Torcassi, C., Schilling, G., Crippen, D., Wood, J. D., Sawa, A., Jenkins, N. A., Copeland, N. G., Borchelt, D. R., Ross, C. A., and Ellerby, L. M. (2006) Progressive phenotype and nuclear accumulation of an amino-terminal cleavage fragment in a transgenic mouse model with inducible expression of full-length mutant huntingtin. *Neurobiol. Dis. 21*, 381−391.
(14) Hackam, A. S., Hodgson, J. G., Singaraja, R., Zhang, T. Q., Gan, L., Gutekunst, C. A., Hersch, S. M., and Hayden, M. R. (1999) Evidence for both the nucleus and cytoplasm as subcellular sites of pathogenesis in Huntington's disease in cell culture and in transgenic mice expressing mutant huntingtin. *Philos. Trans. R. Soc., B 354*, 1047−1055.
(15) Xia, J., Lee, D. H., Taylor, J., Vandelft, M., and Truant, R. (2003) Huntingtin contains a highly conserved nuclear export signal. *Hum. Mol. Genet. 12*, 1393−1403.
(16) Panov, A. V., Gutekunst, C. A., Leavitt, B. R., Hayden, M. R., Burke, J. R., Strittmatter, W. J., and Greenamyre, J. T. (2002) Early mitochondrial calcium defects in Huntington's disease are a direct effect of polyglutamines. *Nat. Neurosci. 5*, 731−736.
(17) Choo, Y. S., Johnson, G. V., MacDonald, M., Detloff, P. J., and Lesort, M. (2004) Mutant huntingtin directly increases susceptibility of mitochondria to the calcium-induced permeability transition and cytochrome c release. *Hum. Mol. Genet. 13*, 1407−1420.
(18) Atwal, R. S., Desmond, C. R., Caron, N., Maiuri, T., Xia, J. R., Sipione, S., and Truant, R. (2011) Kinase inhibitors modulate huntingtin cell localization and toxicity. *Nat. Chem. Biol. 7*, 453−460.
(19) Gu, X. F., Greiner, E. R., Mishra, R., Kodali, R., Osmand, A., Finkbeiner, S., Steffan, J. S., Thompson, L. M., Wetzel, R., and Yang, X. W. (2009) Serines 13 and 16 Are Critical Determinants of Full-Length Human Mutant Huntingtin Induced Disease Pathogenesis in HD Mice. *Neuron 64*, 828−840.
(20) Kelley, N. W., Huang, X., Tam, S., Spiess, C., Frydman, J., and Pande, V. S. (2009) The predicted structure of the headpiece of the Huntingtin protein and its implications on Huntingtin aggregation. *J. Mol. Biol. 388*, 919−927.
(21) Thakur, A. K., Jayaraman, M., Mishra, R., Thakur, M., Chellgren, V. M., Byeon, I. J., Anjum, D. H., Kodali, R., Creamer, T. P., Conway, J. F., Gronenborn, A. M., and Wetzel, R. (2009) Polyglutamine disruption of the huntingtin exon 1 N terminus triggers a complex aggregation mechanism. *Nat. Struct. Mol. Biol. 16*, 380−389.
(22) Tam, S., Spiess, C., Auyeung, W., Joachimiak, L., Chen, B., Poirier, M. A., and Frydman, J. (2009) The chaperonin TRiC blocks a huntingtin sequence element that promotes the conformational switch to aggregation. *Nat. Struct. Mol. Biol. 16*, 1279−1285.
(23) Ignatova, Z., Thakur, A. K., Wetzel, R., and Gierasch, L. M. (2007) In-cell aggregation of a polyglutamine-containing chimera is a multistep process initiated by the flanking sequence. *J. Biol. Chem. 282*, 36736−36743.
(24) Ellisdon, A. M., Thomas, B., and Bottomley, S. P. (2006) The two-stage pathway of ataxin-3 fibrillogenesis involves a polyglutamine-independent step. *J. Biol. Chem. 281*, 16888−16896.
(25) Bulone, D., Masino, L., Thomas, D. J., Biagio, P. L. S., and Pastore, A. (2006) The Interplay between PolyQ and Protein Context Delays Aggregation by Forming a Reservoir of Protofibrils. *PLoS One 1*, e111.
(26) Ratovitski, T., Gucek, M., Jiang, H. B., Chighladze, E., Waldron, E., D'Ambola, J., Hou, Z. P., Liang, Y. D., Poirier, M. A., Hirschhorn, R. R., Graham, R., Hayden, M. R., Cole, R. N., and Ross, C. A. (2009) Mutant Huntingtin N-terminal Fragments of Specific Size Mediate Aggregation and Toxicity in Neuronal Cells. *J. Biol. Chem. 284*, 10855−10867.
(27) Ratovitski, T., Chighladze, E., Waldron, E., Hirschhorn, R. R., and Ross, C. A. (2011) Cysteine Proteases Bleomycin Hydrolase and Cathepsin Z Mediate N-terminal Proteolysis and Toxicity of Mutant Huntingtin. *J. Biol. Chem. 286*, 12578−12589.
(28) Ader, C., Schneider, R., Seidel, K., Etzkorn, M., and Baldus, M. (2007) Magic-angle-spinning NMR spectroscopy applied to small molecules and peptides in lipid bilayers. *Biochem. Soc. Trans. 35*, 991−995.
(29) Bechinger, B., Resende, J. M., and Aisenbrey, C. (2011) The structural and topological analysis of membrane-associated polypeptides by oriented solid-state NMR spectroscopy: Established concepts and novel developments. *Biophys. Chem. 153*, 115−125.
(30) Vidovic, V., Prongidi-Fix, L., Bechinger, B., and Werten, S. (2009) Production and isotope labeling of antimicrobial peptides in *Escherichia coli* by means of a novel fusion partner that enables high-yield insoluble expression and fast purification. *J. Pept. Sci. 15*, 278−284.
(31) O'Nuallain, B., Thakur, A. K., Williams, A. D., Bhattacharyya, A. M., Chen, S., Thiagarajan, G., and Wetzel, R. (2006) Kinetics and thermodynamics of amyloid assembly using a high-performance liquid chromatography-based sedimentation assay. *Methods Enzymol. 413*, 34−74.
(32) Sugawara, M., Resende, J. M., Mendonca Moraes, C., Marquette, A., Chich, J. F., Metz-Boutigue, M. H., and Bechinger, B. (2010) Membrane structure and interactions of human Catestatin by multidimensional solution and solid-state NMR spectroscopy. *FASEB J. 24*, 1737−1746.
(33) Verly, R. M., Moraes, C. M., Resende, J. M., Aisenbrey, C., Bemquemer, M. P., Pilo-Veloso, D., Valente, A. P., Alemida, F. C., and Bechinger, B. (2009) Structure and membrane interactions of the antibiotic peptide dermadistinctin k by solution and oriented ^{15}N and ^{31}P solid-state NMR spectroscopy. *Biophys. J. 96*, 2194−2202.
(34) Bechinger, B., and Aisenbrey, C. (2011) Equilibria governing the membrane insertion of polypeptides and their interactions with other biomacromolecules. In *Thermodynamics/Book 2* (Zgela, V., Ed.) ISBN 978-953-307-978-3.
(35) Vogt, T. C. B., and Bechinger, B. (1999) The interactions of histidine-containing amphipathic helical peptide antibiotics with lipid bilayers: The effects of charges and pH. *J. Biol. Chem. 274*, 29115−29121.
(36) Aisenbrey, C., Bertani, P., and Bechinger, B. (2010) Solid-state NMR investigations of membrane-associated antimicrobial peptides. In *Antimicrobial Peptides* (Guiliani, A., and Rinaldi, A. C., Eds.) pp 209−233, Humana Press, Totowa, NJ.
(37) Salnikov, E., Aisenbrey, C., Balandin, S. V., Zhmak, M. N., Ovchinnikova, A. Y., and Bechinger, B. (2011) Structure and alignment of the membrane-associated antimicrobial peptide arenicin by oriented solid-state NMR spectroscopy. *Biochemistry 50*, 3784−3795.
(38) Aisenbrey, C., and Bechinger, B. (2004) Tilt and rotational pitch angles of membrane-inserted polypeptides from combined ^{15}N and ^{2}H solid-state NMR spectroscopy. *Biochemistry 43*, 10502−10512.

(39) Bechinger, B., and Salnikov, E. S. (2012) The membrane interactions of antimicrobial peptides revealed by solid-state NMR spectroscopy. *Chem. Phys. Lipids 165*, 282−301.
(40) Salnikov, E., Bertani, P., Raap, J., and Bechinger, B. (2009) Analysis of the amide ^{15}N chemical shift tensor of the C_α tetrasubstituted constituent of membrane-active peptaibols, the α-aminoisobutyric acid residue, compared to those of di- and tri-substituted proteinogenic amino acid residues. *J. Biomol. NMR 45*, 373−387.
(41) Batchelder, L. S., Niu, H., and Torchia, D. A. (1983) Methyl reorientation in polycrystalline amino acids and peptides: A ^2H NMR spin lattice relaxation study. *J. Am. Chem. Soc. 105*, 2228−2231.
(42) Strandberg, E., Esteban-Martin, S., Salgado, J., and Ulrich, A. S. (2009) Orientation and dynamics of peptides in membranes calculated from ^2H-NMR data. *Biophys. J. 96*, 3223−3232.
(43) Bechinger, B. (2004) Membrane-lytic peptides. *Crit. Rev. Plant Sci. 23*, 271−292.
(44) Bechinger, B., and Sizun, C. (2003) Alignment and structural analysis of membrane polypeptides by ^{15}N and ^{31}P solid-state NMR spectroscopy. *Concepts Magn. Reson. 18A*, 130−145.
(45) Aisenbrey, C., Sizun, C., Koch, J., Herget, M., Abele, U., Bechinger, B., and Tampe, R. (2006) Structure and dynamics of membrane-associated ICP47, a viral inhibitor of the MHC I antigen-processing machinery. *J. Biol. Chem. 281*, 30365−30372.
(46) Resende, J. M., Mendonca Moraes, C., Munhoz, V. H. D. O., Aisenbrey, C., Verly, R. M., Bertani, P., Cesar, A., Pilo-Veloso, D., and Bechinger, B. (2009) Membrane structure and conformational changes during bilayer-association of the antibiotic heterodimeric peptide distinctin by oriented solid-state NMR spectroscopy. *Proc. Natl. Acad. Sci. U.S.A. 106*, 16639−16644.
(47) DiFiglia, M., Sapp, E., Chase, K., Schwarz, C., Meloni, A., Young, C., Martin, E., Vonsattel, J. P., Carraway, R., Reeves, S. A., et al. (1995) Huntingtin is a cytoplasmic protein associated with vesicles in human and rat brain neurons. *Neuron 14*, 1075−1081.
(48) Gutekunst, C. A., Li, S. H., Yi, H., Ferrante, R. J., Li, X. J., and Hersch, S. M. (1998) The cellular and subcellular localization of huntingtin-associated protein 1 (HAP1): Comparison with huntingtin in rat and human. *J. Neurosci. 18*, 7674−7686.
(49) Zuccato, C., Valenza, M., and Cattaneo, E. (2010) Molecular Mechanisms and Potential Therapeutical Targets in Huntington's Disease. *Physiol. Rev. 90*, 905−981.
(50) Kim, M. W., Chelliah, Y., Kim, S. W., Otwinowski, Z., and Bezprozvanny, I. (2009) Secondary structure of Huntingtin amino-terminal region. *Structure 17*, 1205−1212.
(51) Salnikov, E. S., Mason, A. J., and Bechinger, B. (2009) Membrane order perturbation in the presence of antimicrobial peptides by ^2H solid-state NMR spectroscopy. *Biochimie 91*, 743.
(52) Bechinger, B. (2009) Rationalizing the membrane interactions of cationic amphipathic antimicrobial peptides by their molecular shape. *Curr. Opin. Colloid Interface Sci. 14*, 349−355.
(53) Seelig, J. (2004) Thermodynamics of lipid-peptide interactions. *Biochim. Biophys. Acta 1666*, 40−50.
(54) Wei, S. Y., Wu, J. M., Kuo, Y. Y., Chen, H. L., Yip, B. S., Tzeng, S. R., and Cheng, J. W. (2006) Solution structure of a novel tryptophan-rich peptide with bidirectional antimicrobial activity. *J. Bacteriol. 188*, 328−334.
(55) Abraham, T., Marwaha, S., Kobewka, D. M., Lewis, R. N. A. H., Prenner, E. J., Hodges, R. S., and McElhaney, R. N. (2007) The relationship between the binding to and permeabilization of phospholipid bilayer membranes by GS14dK$_4$, a designed analog of the antimicrobial peptide gramicidin S. *Biochim. Biophys. Acta 1768*, 2089−2098.
(56) Mason, A. J., Martinez, A., Glaubitz, C., Danos, O., Kichler, A., and Bechinger, B. (2006) The antibiotic and DNA-transfecting peptide LAH4 selectively associates with, and disorders, anionic lipids in mixed membranes. *FASEB J. 20*, 320−322.
(57) Sivanandam, V. N., Jayaraman, M., Hoop, C. L., Kodali, R., Wetzel, R., and van der Wel, P. C. (2011) The aggregation-enhancing huntingtin N-terminus is helical in amyloid fibrils. *J. Am. Chem. Soc. 133*, 4558−4566.
(58) Williamson, T. E., Vitalis, A., Crick, S. L., and Pappu, R. V. (2010) Modulation of polyglutamine conformations and dimer formation by the N-terminus of huntingtin. *J. Mol. Biol. 396*, 1295−1309.
(59) Kegel, K. B., Sapp, E., Alexander, J., Valencia, A., Reeves, P., Li, X. Y., Masso, N., Sobin, L., Aronin, N., and DiFiglia, M. (2009) Polyglutamine expansion in huntingtin alters its interaction with phospholipids. *J. Neurochem. 110*, 1585−1597.
(60) Rohl, C. A., Chakrabartty, A., and Baldwin, R. L. (1996) Helix propagation and N-cap propensities of the amino acids measured in alanine-based peptides in 40 volume percent trifluoroethanol. *Protein Sci. 5*, 2623−2637.
(61) Sreerama, N., and Woody, R. W. (2000) Estimation of protein secondary structure from circular dichroism spectra: Comparison of CONTIN, SELCON, and CDSSTR methods with an expanded reference set. *Anal. Biochem.*, 252−260.
(62) Maiuri, T., Woloshansky, T., Xia, J., and Truant, R. (2013) The huntingtin N17 domain is a multifunctional CRM1 and Ran-dependent nuclear and cilial export signal. *Hum. Mol. Genet.*, DOI: 10.1093/hmg/dds554.

NOTE ADDED IN PROOF

Very recently Ray Truant and co-workers showed that Htt17 in addition to its membrane-association capacity also comprises a nuclear export signal at its hydrophobic face.[62]